Electronic Supplementary Material (ESI) for Nanoscale.

Supplementary information:

Out-of-Plane Pressure and Electron Doping Inducing Phase and Magnetic Transition in GeC/CrS_2/GeC van der Waals Heterostructure

Kaiyun Chen[1], *Xue Yan*[2], *Junkai Deng*[3, a)], *Cunle Bo*[3], *Mengshan Song*[1], *Dongxiao Kan*[1], *Jiabei He*[1], *Wangtu Huo*[1] *and Jefferson Zhe Liu*[2, b)]

[1] Northwest Institute for Nonferrous Metal Research, Xi'an 710016, China

[2] Department of Mechanical Engineering, The University of Melbourne, Parkville, VIC 3010, Australia

[3] State Key Laboratory for Mechanical Behavior of Materials, Xi'an Jiaotong University, Xi'an 710049, China

E-mail: [a)]junkai.deng@mail.xjtu.edu.cn; [c)]zhe.liu@unimelb.edu.au

Supplementary Note 1: Lattice constant maching and stacking type between GeC and CrS_2.

In Table S1, we summarized the lattice constants of a series of honey-comb like 2D materials including BN, AIN, GaN, SiC, GeC, graphene, silene and germanene. The lattice mismatch along the *x*- and *y*-direction is defined as $\varepsilon_x = (a\text{-}a_0)/a_0$ and $\varepsilon y = (b\text{-}b_0)/b_0$, where *a* and *b* are the lattice constant of 2D-honeycomb materials. The b_0 =3.325 Å and b_0 = 5.626 Å is the lattice constant of 1T′-CrS_2 along the *x*- and *y*-direction, respectively. The lattice constants of each 2D-honeycomb material and their corresponding mismatch compared to 1T′-CrS_2 are summarized in Table S1. Among these eight candidates, GeC should be the appropriate one for constructing vdWH with CrS_2 because of the smallest mismatch (ε_x = 2.9% and ε_x = 0.6%) compared with other materials.

The stacking type was also considered for vdWH. Based on the relationship between S and Ge atoms, there are three different stacking orders, as shown in Supplementary Fig. S1. The Ge atom might correspond to Cr, top S, and bottom S, respectively. Here, these three stacking types are denoted as Ge-Cr, Ge-S_u, and Ge-S_b, and both single layer and double layer on two sides of CrS_2 are considered. Table S2 summarizes the relative energy of these stacking types. The relative energies of the Ge-S_u stacking in both single and double GeC layer structures are smaller than that of Ge-Cr and Ge-S_d stacking types. Therefore, the Ge-S_u stacking type is adopted in the GeC/CrS_2/GeC vdWHs.

Table S1 The lattice constants of some graphene-like 2D materials. The ε_x and ε_y are the lattice constant mismatch between 2D-honeycomb materials and 1T′-CrS_2 along the *x*- and *y*-direction, respectively.

Lattice constant	BN	AlN	GaN	SiC	GeC	C	Si	Ge
a (Å)	2.503	3.114	3.193	3.093	3.230	2.464	3.868	4.034
b (Å)	4.336	5.393	5.531	5.356	5.595	4.268	6.699	6.986
ε_x (%)	-24.709	-6.343	-3.959	-6.992	-2.842	-25.891	16.323	21.310
ε_y (%)	-22.927	-4.130	-1.689	-4.798	-0.546	-24.133	19.076	24.180

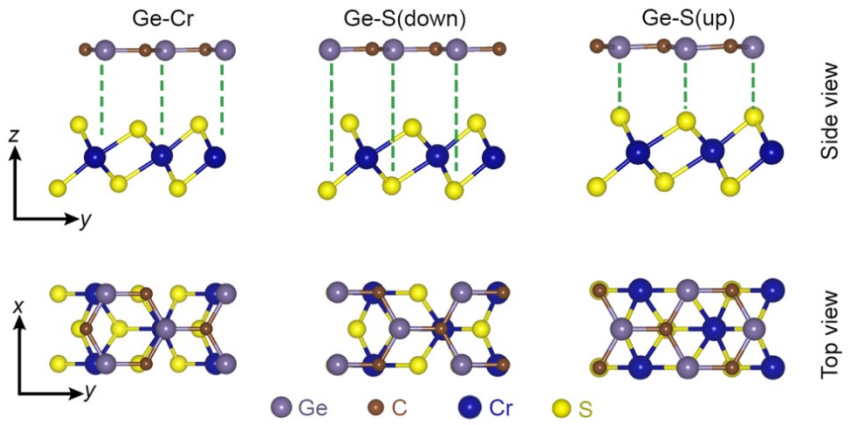

Figure S1 The three possible stacking types of GeC/CrS_2 heterostructure. There is three possible stacking type, of which Ge is on Cr, S (down), and S (up) atom respectively.

Table S2 The energy of different stacking types of GeC/CrS_2 and GeC/CrS_2/GeC van der Waals heterostructure corresponding to Fig. S1. The SL and TL mean the single GeC layer on one side and two GeC layers on two sides.

Energy (eV)	Ge-Cr	Ge-S_u	Ge-S_d
SL	0.125247	0	0.046789
TL	0.245552	0	0.089268

Supplementary Note 2: Energy barriers and phase transition under *out-of-plane* compression

The energy barriers for the phase transition between 1T′-FM and 1T-AFM were calculated through the climbing image nudged elastic band (CI-NEB) method. Considering the CI-NEB is difficult to involve a magnetic transition between AFM and FM, a semi-quantitatively method was adopted to estimate the energy barrier between 1T′-FM and 1T-AFM with and without compression. We first calculated the nonmagnetic 1T-1T′ transition process to approximate transition coordinates. Then self-consistent calculations were performed on each coordinate with AFM and FM magnetic order. The magnetic order with lower total energy at each coordinate is adopted to approximately describe the energy barrier between 1T-AFM and 1T′-FM phase.

Figure S2 is the results of CI-NEB calculations from 1T′-FM to 1T-AFM with d_I = 8.86 Å (relaxed state of GeC/1T′-FM-CrS_2/GeC) and d_I = 8.00 Å (compressed). Obviously, under compression (d_I decreases to 8.00 Å), the energy of 1T′-FM is lower than that of 1T-AFM, and the 1T′-FM to 1T-AFM barrier decreases from 48.1 meV/f.u. to 15.2 meV/f.u., which also suggests the possibility for 1T′-FM to 1T-AFM transition of CrS_2 vdWH.

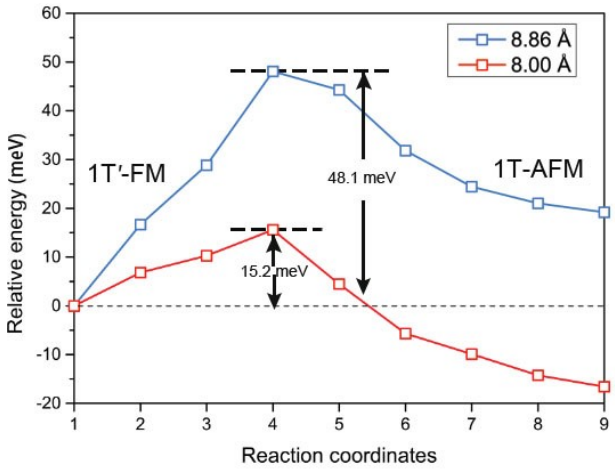

Figure S2 The energy barrier between 1T′-FM and 1T-AFM CrS_2 in GeC/CrS_2/GeC with d_I = 8.86 Å and 8.00 Å.

To identify the phase of CrS_2 in GeC/CrS_2/GeC vdWHs when d_I < 7.74 Å, the distance ratio $d_{Cr1\text{-}Cr2}/d_{Cr2\text{-}Cr3}$ is adopted to identify the structure character (the number of each atoms are denoted in Fig. S3a). Figure S3b depicts the $d_{Cr1\text{-}Cr2}/d_{Cr2\text{-}Cr3}$ of FM-CrS_2 as the function of d_I. The $d_{Cr1\text{-}Cr2}/d_{Cr2\text{-}Cr3}$ slightly increases to ~9.00 as d_I decreases to ~8.00 Å. After that, the abrupt change of

$d_{Cr1\text{-}Cr2}/d_{Cr2\text{-}Cr3}$ to ~0.98 could be observed, and it increases continuously, approaching near 1 as the d_1 decreases. The $d_{Cr1\text{-}Cr2}/d_{Cr2\text{-}Cr3}$ should equal to 1 in the high symmetry 1T phase, while it should be less than 1 in 1T′ phase. Thus, this result suggests the spontaneous phase transition from 1T′ to 1T phase. Here, we also summarized the relationship between the S-Cr-S(Cr-S-Cr) angle of FM-CrS_2 and d_1 as depicted in Supplementary Fig. S3c. All angles abruptly change to ~90º also confirming the 1T′-to-1T transition.

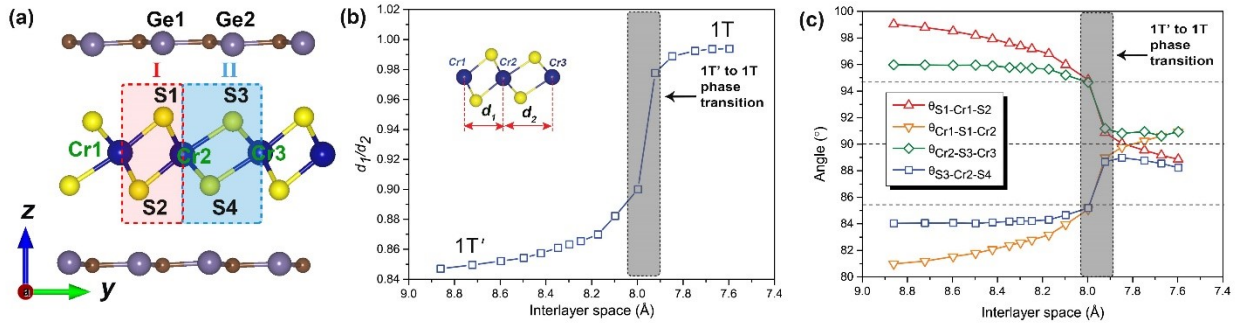

Figure S3 The structure parameter changing of FM-CrS_2 in GeC/CrS_2/GeC during the compression. (a) The schematic of the initial crystal of GeC/1T′-CrS_2/GeC vdWHs. (b) The d_1/d_2 ratio of FM CrS_2. (c) The $\theta_{S1\text{-}Cr1\text{-}S2}$, $\theta_{Cr1\text{-}S1\text{-}Cr2}$, $\theta_{S3\text{-}Cr2\text{-}S4}$, $\theta_{Cr2\text{-}S3\text{-}Cr3}$ changing of FM CrS_2 as the interlayer space decreases. The black dot line at 85.4° and 94.6° corresponds to the ground state of monolayer 1T-CrS_2. The sharp change in (b) and (c) highlighted by the gray dot rectangle corresponds to the spontaneous phase transition from 1T′ to 1T.

Supplementary Note 3: The *out-of-plane* compression, electron doping and uniaxial *in-plane* strain of monolayer CrS_2

To identify the indispensability of GeC layers, *i.e.*, interlayer interaction, the *out-of-plane* compression, uniaxial *in-plane* strain and electron doping are adopted to induced phase transition from 1T′-FM to 1T-AFM in monolayer CrS_2 shown in Fig. S4. It can be observed that the 1T′-FM is always energetically favourable compared with 1T-AFM. In addition, we also summarized the d_1/d_2 ration and S-Cr-S angles corresponding to Fig. S4c in Fig. S5a. Only ~0.7% increase of d_1/d_2 ratio is observed with 10% uniaxial tensile strain applied on monolayer 1T′-FM CrS_2. Also, the linear decreased θ_2 and increased θ_1 suggest the S atoms at each sides turn to close each other without change the 1T′ crystal structure.

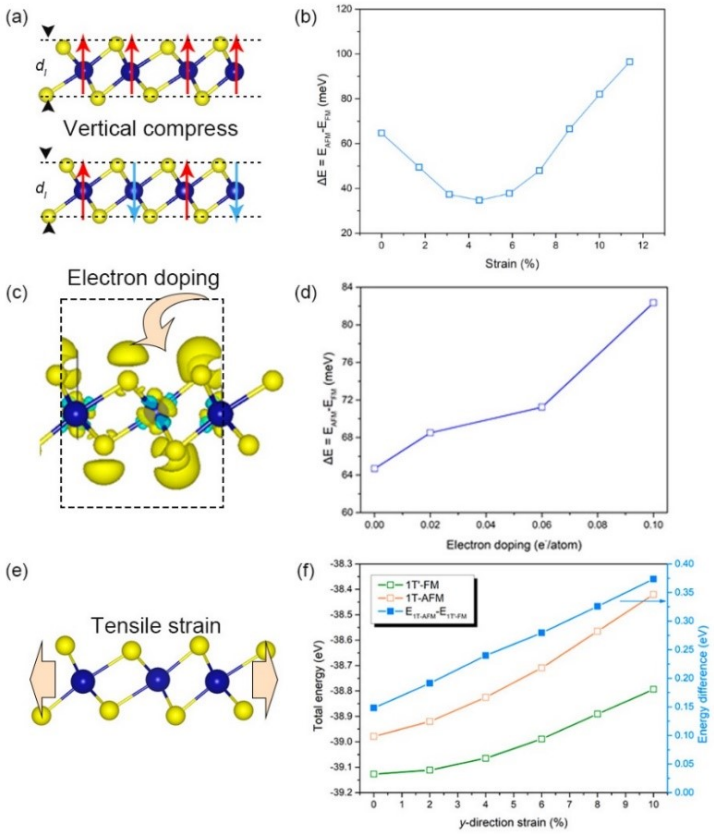

Figure S4 The energy difference between 1T-AFM and 1T′-FM of monolayer CrS_2 as the function of (a)-(b) vertical compression, (c)-(d) electron doping, and (e)-(f) *y*-direction uniaxial strain. 1T′-FM is always the most stable phase without phase transition being observed.

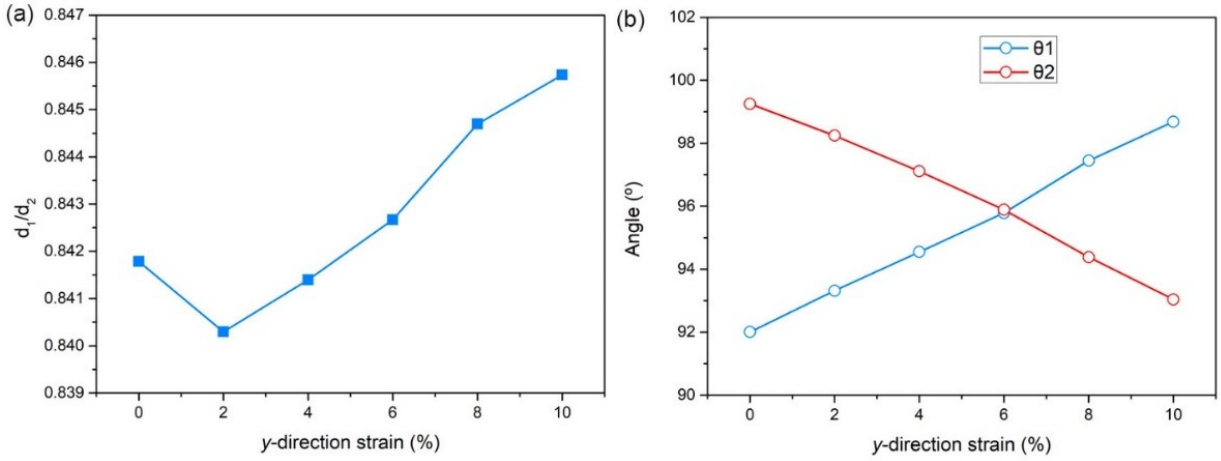

Figure S5 The structure parameters as a function of the *y*-direction tensile strain in 1T′-FM CrS_2. (a) d_1/d_2 ratio, (b) S-Cr-S angle, in which θ_1 and θ_2 corresponds to the inserted figure in Fig. 3c.

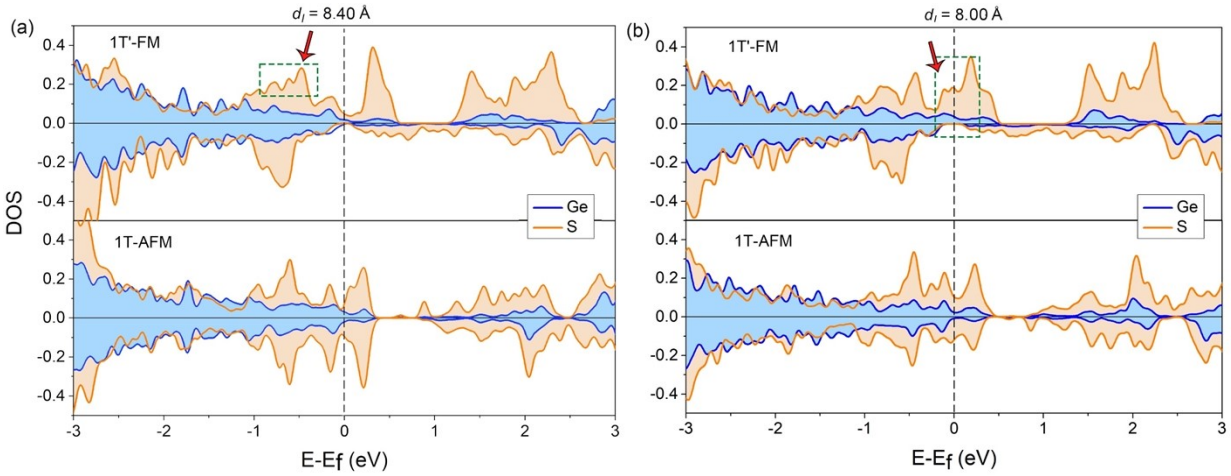

Figure S6 The projected DOS of Ge and S in GeC/CrS_2/GeC with different GeC interlayer distance. (a) is the 1T′-FM and 1T-AFM CrS_2 DOS when d_I = 8.40 Å. (b) is the 1T′-FM and 1T-AFM CrS_2 DOS when d_I = 8.00 Å.

Here, we also calculated the projected DOS (PDOS) of S and Ge in GeC/CrS_2/GeC with d_I = 8.40 Å and 8.00 Å as show in supplementary Fig. S6. At d_I = 8.40 Å, the peak of S in 1T′-FM and 1T-AFM are not well comparatable to Ge, especially the peaks highlighted by the green dot rectangle. In addition, both S and Ge show similar peaks near to the Fermi level. This suggest the weak interaction between S and Ge. As the d_I decreases to 8.00 Å, more electrons concentrate on Fermi level in 1T′-FM CrS_2 as highlighted in the green dot rectangle. Such a state is not energitcal favorable compared to the 1T-AFM of CrS_2, because the DOS intensity will decrease at Fermi

level. In addition, it can be observed that more profound peak overlap as the electron density increases enhancing Ge and S interaction. Therefore, the enhanced interlayer interaction will make the energy of 1T-AFM lower than that of 1T′-FM.

Supplementary Note 4: Calculation of stress-strain curve of GeC/CrS_2/GeC under out-of-plane compression.

To estimate the possible application of the vertical compress-induced phase and magnetic transition, the compressive strain-stress curve should be calculated to identify whether the stress could be realized in experiments. The compressive stress could be estimated through:

$$P = \Delta E/\Delta V \quad (1)$$

where E and V are the total energy and volume of GeC/CrS_2/GeC heterostructure, respectively. The volume could be defined as $V = S \times d_I$, where S is the surface area of GeC/CrS_2/GeC in the x-y plane. The FM state is used to estimate the pressure during the compression process, and the E-V curve is presented in Supplementary Fig. S7. Then the stress–d_I relationship is depicted in Supplementary Fig. S9. It can be observed that ~4.3 GPa is necessary to be applied to trigger 1T′-FM to 1T-AFM (d_I = 8.26 Å) in GeC/CrS_2/GeC vdWH. Furthermore, the stress along the z-direction will increase as the interlayer continue decreasing until a plateau ($\varepsilon \approx 10$ GPa) appears around 8.00 Å, which corresponds to the 1T′-FM to 1T-FM spontaneous transition.

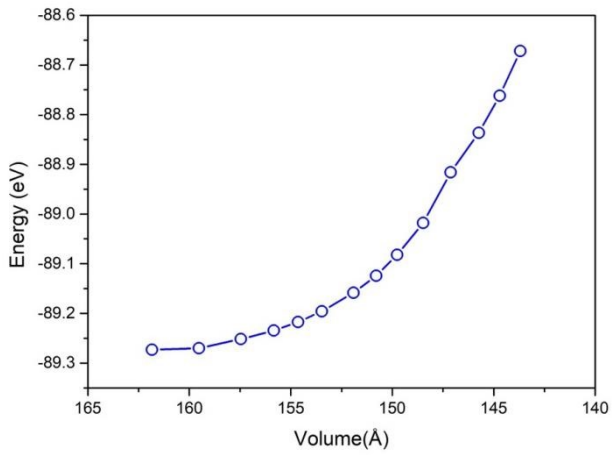

Figure S7 The relationship between total energy and volume of GeC/1T′-FM-CrS_2/GeC.

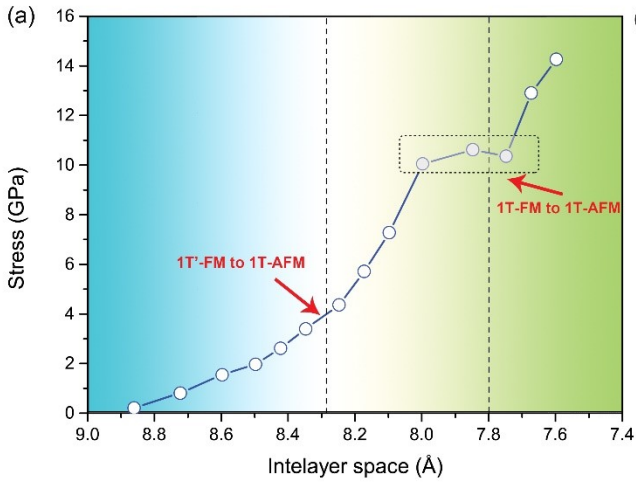

Figure S8 (a) The relationship between stress and GeC interlayer space of GeC/1T′-FM-CrS_2/GeC. The 1T′-FM to 1T-AFM transition stress is ~4.3 GPa. The plateau highlighted by the gray rectangle corresponds to the spontaneous 1T′ to 1T transition.

Supplementary Note 5: Direct-to-super exchange transition inducing the 1T-AFM to 1T-FM transition

For the FM 1T phase at d_I = 8.00 Å, the Cr-X -Cr bond angle is not equal to 90° as shown in Fig. S3. The $\theta_{Cr1\text{-}S1\text{-}Cr2}$ and $\theta_{Cr2\text{-}S3\text{-}Cr3}$ are larger and smaller than 90°. The magnetic moment of S is very close to zero. As reported in previous studies in monolayer CrX_2 (X = S, Se and Te)[1], the AFM state of the 1T phase arises from the direct exchanging interaction (J_D) between the nearest neighbouring Cr atoms as shown in Fig. S9. As the *out-of-plane* compression increase, both $\theta_{Cr1\text{-}S1\text{-}Cr2}$ and $\theta_{Cr2\text{-}S3\text{-}Cr3}$ turn to close to 90°. Considering the number of 3*d* electrons of the Cr atom, it should be the superexchange to direct exchange interaction transition based on the Goodenough-Kanamori-Anderson (GKA) rules[2-4]. The magnetic moment on S is increased from 0 μ_B to –0.02 μ_B, and opposite to the magnetic moment of Cr (2.09 μ_B).

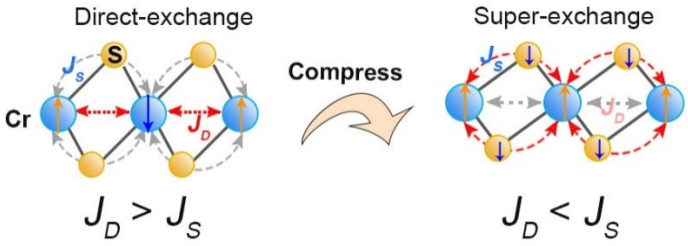

Figure S9 The different exchange interactions in CrS_2. The Cr-Cr direct exchange (J_D) under small compression leads to AFM order, while the Cr-S-Cr superexchange (J_S) under large compression leads to FM. The orange and blue solid arrow represent the magnetic moment with different signals.

Supplementary Note 6: Magnetic moment and relative energy of FM/AFM lateral heterostructure.

Here, we constructed two different superlatice of GeC/CrS_2/GreC, in which the compressed region is 8 and 4 unit cell, respectively. Table S3 summarized the magnetic moment of each Cr atoms in these two superlattice structures. For the 8 units compressed superlattice (4F+8C), Cr1 to Cr4 show FM order in stress free region, while Cr5 to Cr12 show AFM order in compressed region. For the 8 unit compressed superlattice (8F+4C), Cr1 to Cr8 show FM order in stress free region, while Cr9 to Cr12 show AFM order in compressed region. The spin polarized electron density is shown in Fig. 6 in main text.

To indentify the ground state in such vdWH, we manully change the magnetic order of compressed region to FM order. The relative energies are summarized in Table S4. For both two superlattice, the AFM order in compressed region is energetical favorable.

Table S3 Magnetic moment of free and compressed local structure combination with FM+AFM. The magnetic moment of each atom is μ_B.

Atoms	Cr1	Cr2	Cr3	Cr4	Cr5	Cr6	Cr7	Cr8	Cr9	Cr10	Cr11	Cr12
4FM+8AFM	1.777	2.021	2.06	2.121	2.18	-2.138	2.127	-2.126	1.967	-2.05	2.025	-1.984
8FM+4AFM	1.813	1.976	2.114	2.117	2.091	2.137	2.052	2.09	2.178	-2.147	2.107	-1.916

Table S4 The energy of relax and compress local structure combination with FM+AFM and FM magnetic order. The unit of each energy is eV.

*n*F+*m*C	4F+8C	8F+4C
E(nFM+nAFM)	-532.36436	-532.77456
E(nFM+nFM)	-532.25102	-532.74085
$\Delta E(E_{FM+AFM}-E_{FM})$	0.11334	0.03371

References:

1. Lv, H. Y., Lu, W. J., Shao, D. F., Liu, Y. & Sun, Y. P. Strain-controlled switch between ferromagnetism and antiferromagnetism in 1T−CrX_2 (X=Se, Te) monolayers. *Phys. Rev. B* **92** (2015).

2. Anderson, P. W. New approach to the theory of superexchange interactions. *Phys. Rev.* **115**, 2-13 (1959).
3. Goodenough, J. B. Theory of the role of covalence in the perovskite-type manganites [La, M(II)]MnO_3. *Phys. Rev.* **100**, 564-573 (1955).
4. Kanamori, J. Crystal distortion in magnetic compounds. *J. Appl. Phys.* **31**, S14-S23 (1960).